Robotica (2010) volume 28, pp. 171–183. © Cambridge University Press 2009
doi:10.1017/S0263574709990610

A reconfigurable modular robotic endoluminal surgical system: vision and preliminary results

Kanako Harada†,*, Denny Oetomo‡,§, Ekawahyu Susilo†,¶, Arianna Menciassi†,¶, David Daney§, Jean-Pierre Merlet§ and Paolo Dario†

† *CRIM Lab, Scuola Superiore Sant'Anna, Pisa 56025, Italy*
‡ *Department of Mechanical Engineering, University of Melbourne, Victoria 3010, Australia*
§*Project COPRIN, INRIA Sophia-Antipolis FR-06902, France*
¶*The Italian Institute of Technology (IIT), Genova 16163, Italy*

(Received in Final Form: October 27, 2009. First published online: December 10, 2009)

SUMMARY
Miniaturized surgical devices are promising for the future development of minimally invasive and endoluminal surgery. However, the dexterity and therapeutic functions of these devices are limited. In this paper, a reconfigurable modular robotic system is proposed to perform screening and interventions in the gastrointestinal tract. In the proposed system, millimeter-sized robotic modules are ingested and tasked to assemble into an articulated mechanism in the stomach cavity. The modules are assembled according to the target location to perform precise intervention. Based on this concept, a preliminary report is presented covering the robotic schemes for the endoluminal reconfigurable platform, the design with structural functions, the control strategy, and the interval-based constraint satisfaction algorithm to determine the suitable topologies of the reconfigurable robot for the given task.

KEYWORDS: Modular robot; Surgical robot; Mechanical design; Endoluminal surgery; Interval analysis.

1. Introduction

Surgical robots have been widely accepted in the last decade and contributed to the development of minimally invasive surgery. Concerning diagnosis and therapy in the gastrointestinal (GI) tract, the trend of surgical robots is going from teleoperated master-slave manipulators to miniaturized endoluminal devices.[1] Capsule endoscopy[2] is one example of such diagnosis and it has been performed worldwide in the last five years with successful outcomes. Commercial capsule endoscopes have generally no locomotive and therapeutic functions; therefore, in order to improve the controllability and precision of the diagnosis, functionalized endoluminal devices have been studied, including legged capsules,[3] pneumatically actuated endoluminal devices with inchworm-type locomotion,[4] locomotive capsules driven by external magnetic fields,[5] and micro actuators for miniaturized surgical devices.[6–8] Moreover, endoluminal mobile robots for biopsy[9] have been demonstrated in the new surgical procedure called Natural Orifice Translumenal Endoscopic Surgery (NOTES),[10] where the surgical tools are inserted from a body's natural opening to approach the target organ, hence eliminating skin incisions. These devices are promising for the future development of minimally invasive and endoluminal surgery. However, the dexterity and therapeutic function of these devices are limited mainly because of the size constraints and geometry of the traditional endoscopic devices.

In this paper, a reconfigurable modular robotic system is proposed to perform screening and interventions of the GI tract. In the proposed system, small-scaled robotic modules are ingested and assembled to form an articulated structure in the stomach.[11] The way the robot is assembled from individual modules depends on the target location and required surgical tasks. This approach is appealing for next generation surgical robots as well as for applications of reconfigurable modular robots. Reconfigurable modular robots[12, 13] have been studied to be potentially more robust and more adaptive to the working environment. These features can also benefit the surgical applications by considering the intricate intracorporeal workspace. At present, there have been no reconfigurable modular robots for surgical use reported in the literature to the best of the authors' knowledge. The smallest state-of-the-art reconfigurable modular robot reported in literature is composed of wired modules, each of size 20 mm cube,[14] which is too big for the patients to ingest; therefore, the modular miniaturization down to the ingestible size is one of the most challenging goals for endoluminal application. High-level challenges also exist in determining the suitable topology that the modules can be assembled to, given the task requirements. From the modular robotics research viewpoint, the proposed system is unique as it has a very specific and focused application to the surgical procedures and the GI tract environment. This poses a strict set of task requirements associated with the robotic design. Establishment of a numerical methodology to certify whether the task requirements can be satisfied for a modular robotic topology, given the design and environment limitations,

* Corresponding author. E-mail: k.harada@sssup.it

would be useful for this surgical system. Moreover, the methodology can be adapted to any modular robot given a specific application.

Based on this background, the current paper is organized as follows. Section 2 describes the concept of the surgical system, the target pathologies, and the proposed schemes for the endoluminal reconfigurable robotic system. Section 3 and Section 4 report the design of the modules for the proposed robotic schemes and their prototypes. Section 5 illustrates the control strategy of the entire system and Section 6 details the methodology to determine the suitable robot topology to carry out the given tasks. Finally, the results and future work are discussed in Section 7 and Section 8 respectively.

2. Reconfigurable Modular Robot for Endoluminal Surgical System

2.1. Concept of the System

The modular architecture was selected to overcome the intrinsic limitations of current capsule endoscopy as it allows the delivery of more components inside the human body with different or similar functions. Based on this concept, the patient ingests some capsular modules consisting of modules with structural functions and modules with diagnostic and/or interventional functions. The modules for diagnosis are equipped with a camera or a biochemical sensor, while the interventional modules are endowed with surgical tools such as forceps. A wireless camera, such as the one used for commercial capsules, can be integrated into a module to provide real-time image both for diagnosis and intervention.

Using preoperative imaging data, the robotic workspace inside the GI tract is defined and the modular assembly of the possible robotic topologies is calculated. The assembly, the robotic configuration, and the surgical tasks are controlled via wireless bidirectional communication with an external console operated by the surgeon, while the progress in procedure is observed by using intraoperative imaging devices. For example, 3D fluoroscopy can provide the shape of the stomach during the operation and can localize the robot in the GI tract, while the ingested camera module(s) can help visualize the target site of the stomach and the surgical task done by the interventional modules. After the surgical tasks are completed, the robot disassembles itself into individual modules or reconfigures itself into another shape that is adequately small/narrow to pass through natural orifices and finally to exit the body.

2.2. Clinical target and constraints

The clinical target for the proposed surgical system is identified as the entire GI tract, i.e., the esophagus, the stomach, the small intestine, and the colon. After the detailed analysis of the GI anatomy, the pathological syndromes which can benefit from the reconfigurable surgical robot were investigated. In summary, the colon appears to have the largest potential of clinical impact due to cancer high incidence ratio, while a modular surgical robot able to reach the small intestine has the greatest novelty. The stomach is the easiest target due to its relatively large working space, but it is still very interesting and challenging from the diagnostic viewpoint. In fact, stomach cancer is the second leading cause of cancer death worldwide and accounts for almost one million deaths per year.[15] As a delayed diagnosis may lead to poor prognosis, early diagnosis and therapy utilizing advanced endoluminal devices are desirable.

The location of the stomach cancer is known to affect a five-year survival rate as reported in literature,[16] which shows worse outcomes in cases where the cancer is located in the upper side of the stomach. The current endoscopic capsules are not capable of reaching this district due to the absence of locomotion ability, but the actuated modular surgical robot can be deployed to perform accurate diagnosis and intervention at this specific site. Thus, the development of a reconfigurable robot that assembles in the stomach is thought to be a good proof-of-concept. The first target task for the proposed surgical system is then defined as the biopsy of cancer in the upper side of the stomach, called the *Fundus* and the *Cardia*: the fundus is the rounded upper end of the stomach and the cardia is located at the gastroesophageal junction.

The stomach is essentially an elastic bag having a volume of 50 mL when empty and it can distend up to a volume of 1400 mL when full. The thickness of the gastric wall ranges between 2.35 mm and 5.43 mm[17] and its inner surface is characterized by many gastric folds. For this reason, the stomach must be inflated with either air or liquid, or stretched by robotic arms as part of a surgical procedure to expose the entire internal surface.

Although the stomach has a large workspace, each module of the reconfigurable system should be small enough to be swallowed: a capsule module 8 mm in diameter and 16 mm in length can be swallowed comfortably by $80-90\%$ of people and it can pass through the whole GI tract without problems. The proposed surgical system aims to finally achieve this target dimension. At the moment, the current prototypes reported in this paper are of dimension 13 mm in diameter and 23 mm in length for the homogeneous scheme and 15.4 mm in diameter and 36.5 mm for the heterogeneous scheme. Meanwhile, the size of commercially available endoscopic capsules is 11 mm in diameter and 26 mm in length;[2] this size has been shown to be acceptable for the majority as an ingestible device. Thus, this specification is mandatory to be used in clinical cases.

2.3. Robotic scheme

As the proposed surgical system imposes many peculiar constraints that have rarely been discussed in the design of modular robots, two robotic schemes are being proposed and investigated in parallel. This enables us to gain insights and indications to design rules/guidelines as well as the strength and weaknesses of the design schemes. Regardless of the robotic scheme, each module was designed to contain one or two motors, a control board, and a battery inside. The control board embedded in each module is capable of wireless communication to receive commands from an external console operated by the surgeons. The control scheme is described in Section 5.

The first robotic scheme to be analyzed is the homogeneous scheme (Fig. 1a), where all modules are identical except for one or two surgical or diagnostic modules. In this scheme, the

https://doi.org/10.1017/S0263574709990610 Published online by Cambridge University Press

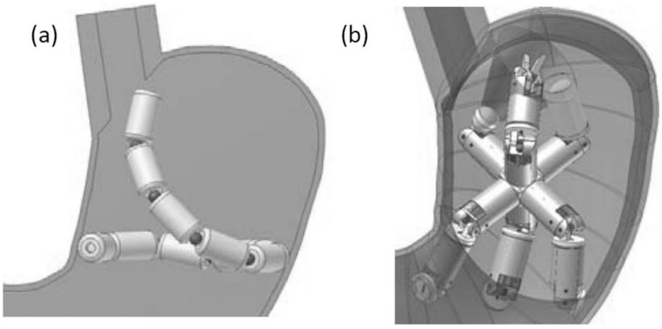

Fig. 1. Robotic schemes: (a) homogeneous scheme and (b) heterogeneous scheme for the endoluminal reconfigurable platform.

assembly is not critical because the modules can be connected without considering a specific sequential conjunction nor orientation of each module. After all modules are connected, the modules next to the other are identified by the internal communication which has not yet been implemented in the design reported in this paper. Because the topology of the robot in this homogeneous scheme is limited to a serial chain, the topology planning and control are less complex. On the other hand, this scheme is adequate only for a simple surgical task. Thus, the advantage of this scheme is the simplicity in assembly, in determining the topology of the assembled robot, and in control method. The main weakness is that it is effective only for simple tasks.

The second robotic scheme is the heterogeneous scheme (Fig. 1b). It consists of one or more central branching module(s), structural modules, and additional functional modules. With this geometry, surgical tasks requiring a more advanced kinematics and a specific target approach can be performed. On the other hand, the assembly is more difficult because the assembling sequence should be preplanned and realized remotely. In this scheme, the robot has a variety of topologies that can be realized through reconfiguration, by repeated docking and undocking of the modules. The ability to supply more specific modules gives the advantage of a more capable robotic system, with the obvious trade-off of increased system complexity.

2.4. *Surgical procedures*

The steps in the surgical procedures to be carried out are almost the same between the two robotic schemes and are proposed in Fig. 2. Prior to the surgical procedure, the patient distends the stomach by drinking a liquid. This liquid also acts as a medium for floating the robotic modules to form a rigid structure before beginning intervention or diagnosis (Fig. 2b). The liquid provides a large space to allow 2-dimensional assembly of 10–15 floatable modules on its surface. The surface of the filled liquid is about 100 mm in diameter, thus allowing the assembly of the floatable modules (Fig. 2c). The swallowed modules complete the assembling process before the liquid naturally drains away from the stomach, which is in a window of 10–20 min (Fig. 2d). Soon after, the assembled robot configures as planned based on preoperative diagnosis, in order to perform the detailed examination and intervention (Fig. 2e). In the homogeneous scheme, the docking is completed when the modules are connected into the desired serial chain with the planned number of modules. In the heterogeneous scheme, repeated docking and undocking between the modules may be necessary until the planned topology is achieved. After the surgical tasks are completed, the robot reconfigures itself to a snake-like shape to pass through the pyloric sphincter (Fig. 2f), or disassembles itself into individual modules (Fig. 2g).

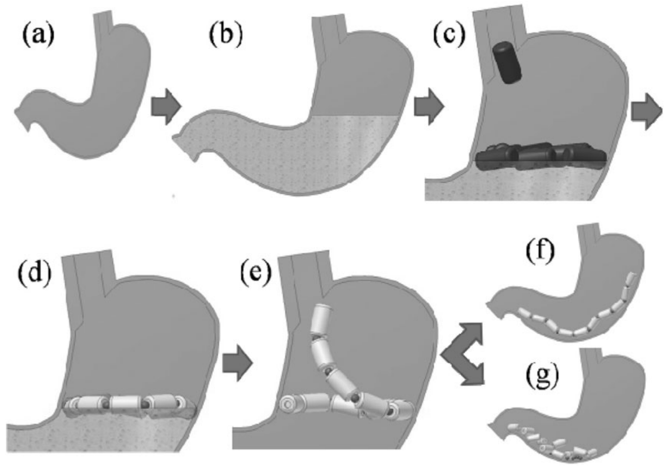

Fig. 2. The proposed procedures: (a) empty stomach, (b) stomach filled with a liquid, (c) ingested capsules on the liquid surface, (d) assembled modules, (e) robotic configuration and diagnosis/intervention, (f) reconfiguration to a snake-like topology, and (g) disassembled modules.

3. Design of a Structural Module for the Homogeneous Scheme

3.1. *Design of bending module for the homogeneous scheme*

Any reconfiguration process is enabled by endowing modules with actuated bending mechanisms, thus allowing them to approach other modules. To set up the robot in the homogeneous scheme, subcomponents for energy storage/power supply, actuation, and control are incorporated into all modules. Figure 3 shows the design of the bending module that the authors have conceived for this scheme.[18] Each module is identical and docked using one NdFeB spherical magnet (K-06-C Webcraft GmbH, Switzerland) to have 2 DOF bending of 30° in each direction at the docked joint. Each module contains also a Li-Po battery (LP2-FR, Plantraco Ltd., Canada), a DC brushless motor 2.4 mm in diameter (SBL02-06H1PG337, Namiki Precision Jewel Co., Ltd., Japan) and a custom-made motor control board which enables wireless communication (see Section 5 for more details).

The design utilizes the motor to drive a mechanism, formed by two parallel struts moving up and down as shown in Fig. 3. When this actuated end of the module is docked to another bending module on the actuated end, a 2 DOF bending motion is obtained, where the axes of the 2 DOF rotation intersect at the center of the spherical magnet. The two parallel struts exhibit a translational motion to push the surface of the docked module, resulting in $\pm 30^{\circ}$ of bending (maximum).

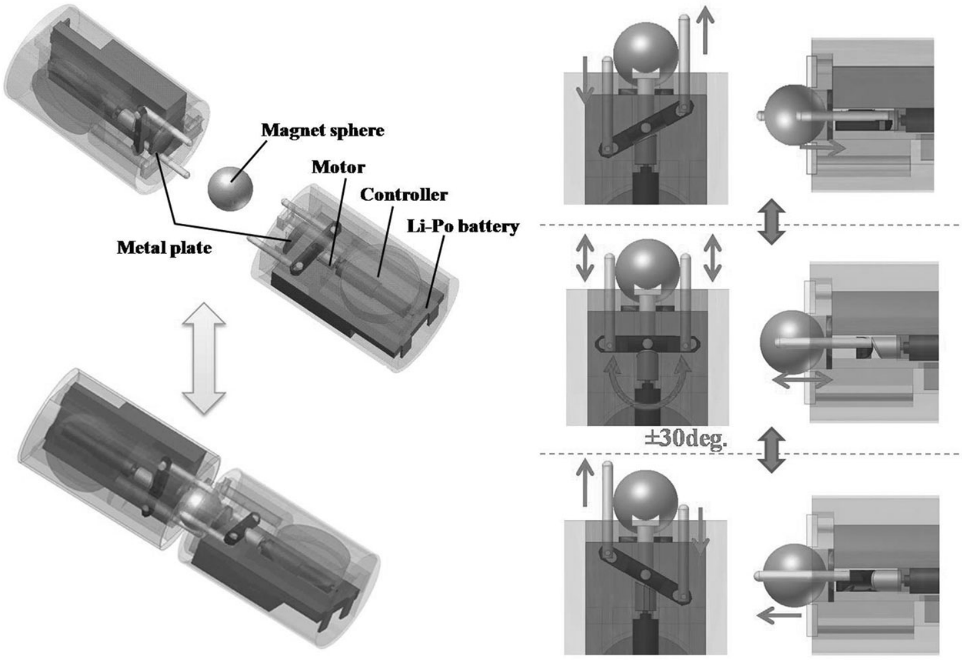

Fig. 3. Design of the bending module for the homogeneous scheme.

The two modules are kept together by the spherical magnet. The module is 13 mm in diameter and 23 mm in length, which is a little larger than the commercial endoscopic capsule (11 mm in diameter and 26 mm in length) whose size is defined as mandatory for clinical use.

3.2. Design of the bending mechanism

The 2 DOF bending at the joint is achieved by docking two identical 1 DOF mechanisms that share the center of the sphere magnet. The design of the 1 DOF bending mechanism is illustrated in Fig. 4. The joint bends around the center O_1, which is the center of the spherical magnet. Two struts are kept parallel and translated with distal ends in contact with the surface of the other module. The shafts at proximal ends slide in the holes of the bar that rotates around O_2. The gap between the modules with a null bending is given by:

$$k = \sqrt{{D_1}^2 - {D_2}^2} \tag{1}$$

where D_1 is the diameter of the spherical magnet and D_2 is the diameter of the hole whose edge fits the sphere. Each strut has a length l and a hemispherical shape with radius r at its ends. Therefore, the maximum distance between the modular end plane and the proximal end of the strut is the following:

$$d = l + r - k \tag{2}$$

The distance between O_2 and the proximal end of the strut is given by:

$$b = \frac{a}{\cos\theta} \tag{3}$$

where θ is the bending angle of the joint and a is the distance between O_2 and the central axis of the strut. The amount of

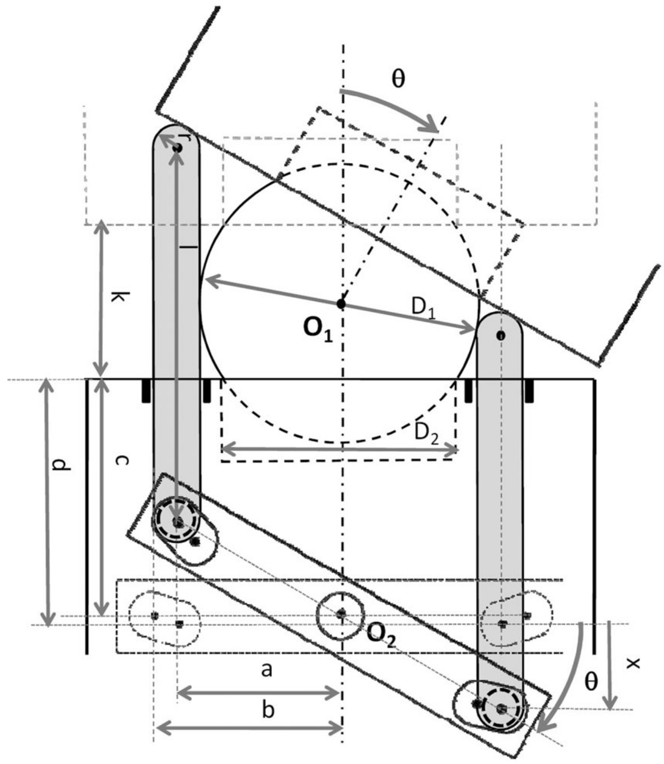

Fig. 4. Side view of the bending mechanism showing design parameters for a 1 DOF bending.

translational movement of the strut x is given by:

$$x(\theta) = \frac{k}{2}(1 - \cos\theta) + \left(a - \frac{k}{2}\sin\theta\right)\tan\theta - r\left(1 - \frac{1}{\cos\theta}\right) \tag{4}$$

https://doi.org/10.1017/S0263574709990610 Published online by Cambridge University Press

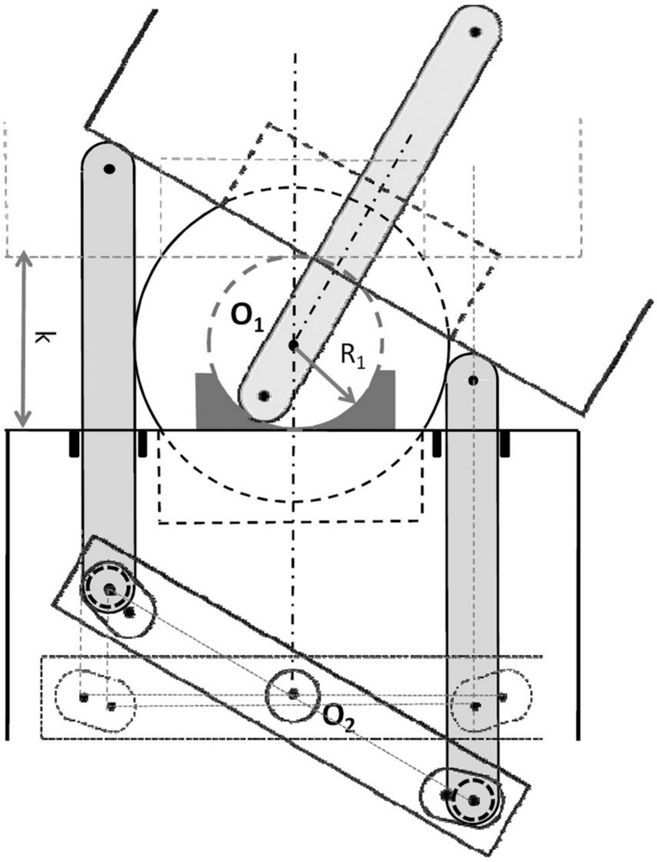

Fig. 5. Side view of the bending mechanism showing the concave part of the 2 DOF bending module.

The distance between O_2 and the modular end plane is given by:

$$c = d - b\sin\theta + x(\theta) \quad (5)$$

Based on the selected design, θ has the displacement range of

$$-\frac{1}{6}\pi \leq \theta \leq \frac{1}{6}\pi \quad (6)$$

Two identical mechanisms are then combined to achieve 2 DOF of bending that share the same rotation center (O_1). To keep all distal ends of the four struts in contact with the surface of the docked module, a concave part was designed as shown in Fig. 5. The curvature radius of the concave part is given by:

$$R_1 = \frac{k}{2} \quad (7)$$

For the first prototype of the 1 DOF bending mechanism, Table I reports the most important parameters, selected or derived. The b and the c parameters give the dimension of the holes of the bar.

3.3. Prototyping

Figure 6 shows the fabricated prototypes of the bending module. The casing was fabricated by 3D printing (InVision XT 3-D Modeler, 3D systems, Inc., USA). The struts and the concave parts are made of conductive and nonmagnetic material to be potentially used for the electrical connection between the modules internal communication. The spherical magnet is made of Neodymium–Iron–Boron (NdFeB), having enough force to dock the modules. The experiments to evaluate the torque and the positioning accuracy will be performed after the implementation of the motor control described in Section 5.

Table I. Parameters for the bending mechanism, in millimeters.

Selected parameters		Derived parameters	
D_1	6.0	k	3.32
D_2	5.0	d	5.18
l	8.0	b_{max}	4.04
r	0.5	c_{min}	5.00
a	3.5	R_1	1.66

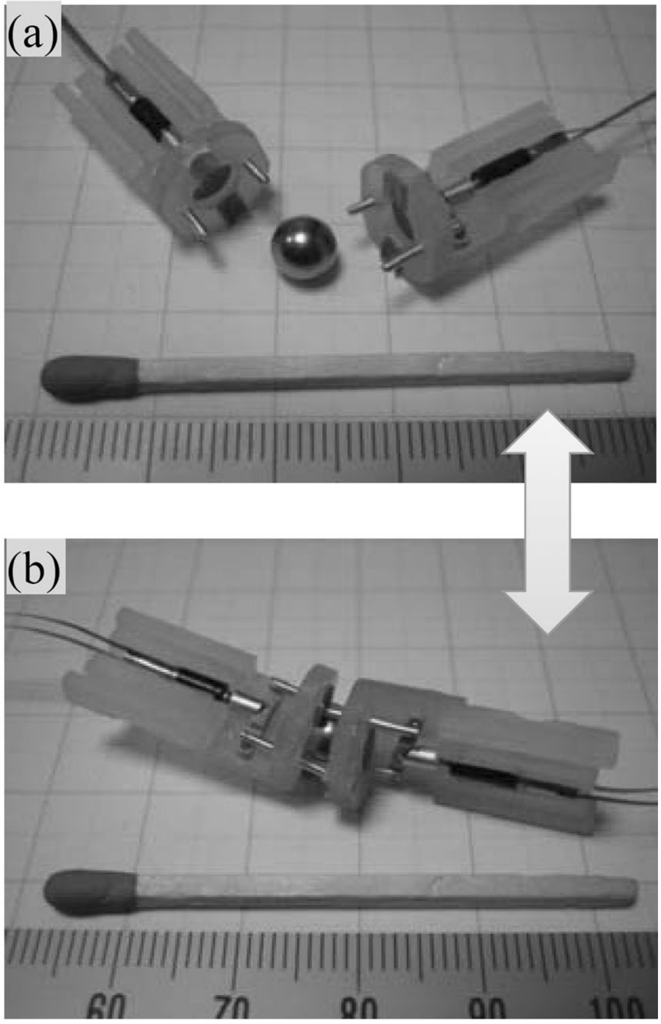

Fig. 6. Homogeneous scheme: prototypes of the bending module: (a) undocked modules and (b) docked modules.

4. Design of a Structural Module for the Heterogeneous Scheme

4.1. Schematic design

Possible modular configurations for the heterogeneous robotic scheme are illustrated in Fig. 7. The designed robotic

https://doi.org/10.1017/S0263574709990610 Published online by Cambridge University Press

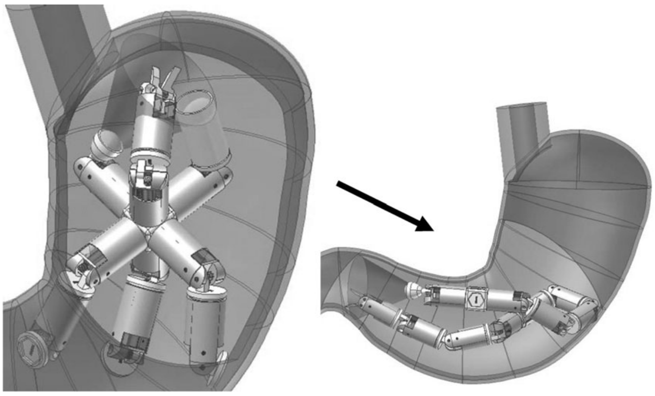

Fig. 7. Example of the reconfiguration feature.

configurations are composed of 12 modules: one camera module with LEDs for illumination, one biopsy module to cut the tissue, one storage module to carry the sampled tissues out of the body, one central passive module able to contain an extra battery, and eight active modules. The design of the active module with 2 DOF ($\pm 90^\circ$ of bending and 360° of rotation) is shown in Fig. 8. The bending mechanism is composed of a worm gear and a spur gear (9:1 gear reduction), whereas the rotation mechanism is composed of two spur gears (no gear reduction). All gears are purchased from DIDEL (DIDEL SA, Switzerland) and the width and/or length were modified by additional machining. The final module size is 15.4 mm in diameter and 36.5 mm in length which is larger than the defined specification. The main constrains were the size of the commercially available components. It contains a Li-Po battery, two DC brushless motors of 4 mm in diameter (SBL04-0829PG337), and a custom-made motor control board. The choice of the motors will be further iterated after the analysis of the design

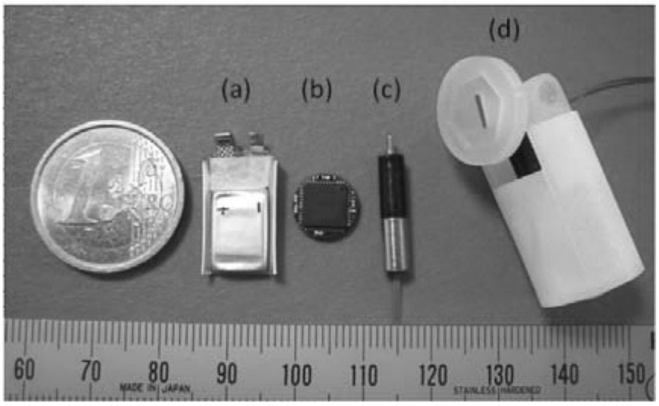

Fig. 9. Components for the heterogeneous module (a) Li–Po battery, (b) custom-made control board, (c) DC brushless motor with 4-mm diameter and (d) casing.

parameters and the evaluation of the prototypes with respect to the given tasks. Two permanent magnets (Q-05-1.5-01-N, 5 mm × 1.5 mm × 1 mm) are attached at each end of the module to help self-alignment and modular docking. The smallest magnet having enough force to lift at least two modules was chosen; however the force produced by these magnets is not enough for self-assembly. The possibility of magnetic self-assembly using permanent magnets has been demonstrated in literature[19] and the adequate choice of the magnets are being investigated to maximize the possibility of self-assembly.

4.2. *Prototyping*

The prototyping process to produce the heterogeneous modules were carried out in the same manner as that for the homogenous scheme. The components assembled into one module are shown in Fig. 9. The assembled module are

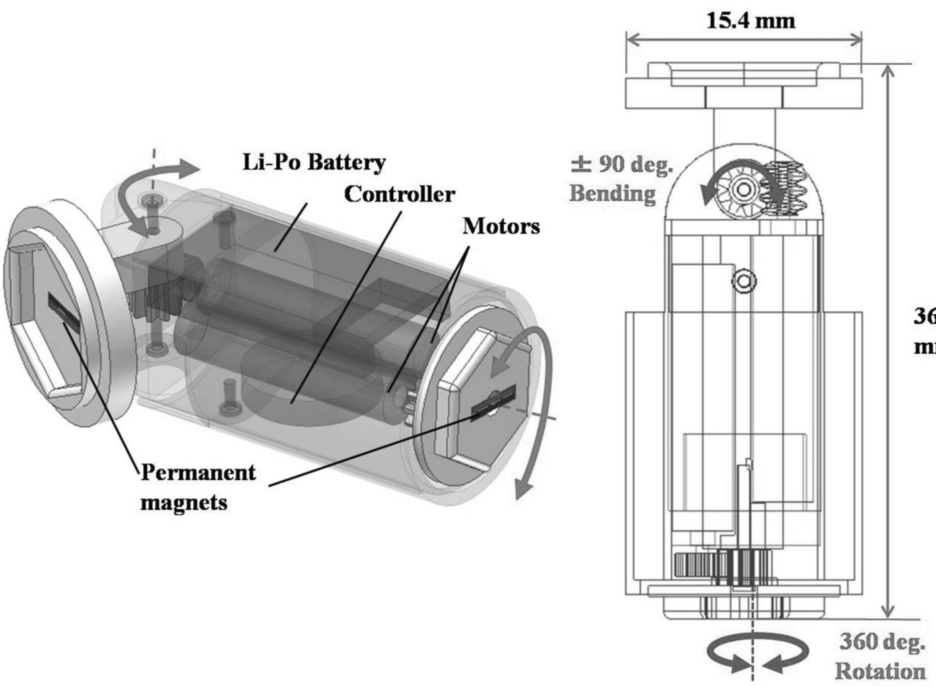

Fig. 8. Design of the heterogeneous module.

https://doi.org/10.1017/S0263574709990610 Published online by Cambridge University Press

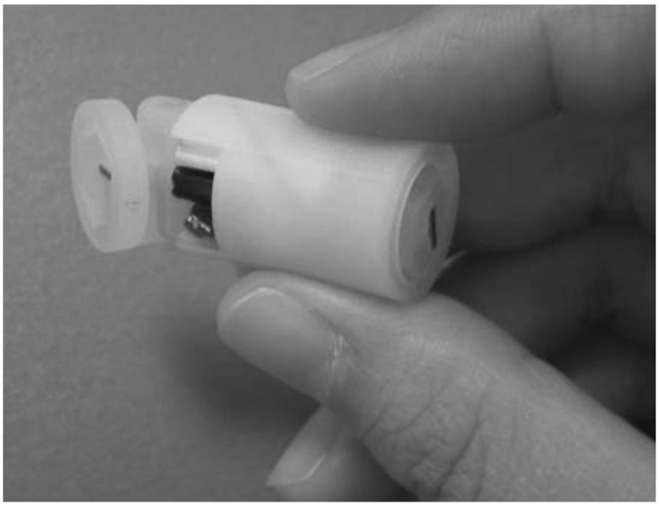

Fig. 10. Heterogeneous scheme: prototype with all the components assembled.

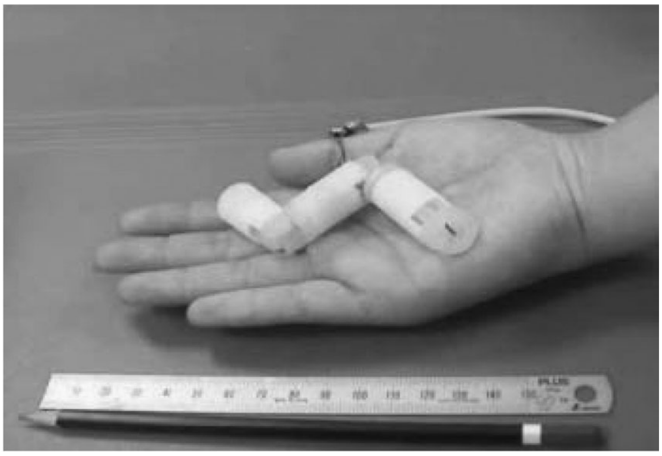

Fig. 11. Docked modules in the heterogeneous scheme.

shown in Fig. 10 and three modules attached together are shown in Fig. 11.

5. Control Strategy and Power Management

5.1. *Overall control strategy*

To simplify the hardware design and modularity, a standard control board is to be used in all modules, regardless of their intended functionalities, in both the homogeneous and heterogeneous schemes. This control board was developed in-house and it has a programmable microcontroller, which needs to be programmed specific to the function of the module and the types of peripherals attached. For example, the bending module has a brushless DC motor as its peripherals, and the diagnostic module is equipped with a camera. Consequently, each module of the proposed system has the same control board with function specific algorithms loaded to the program memory of the microcontroller.

5.2. *Control board development*

The realization of the control system started from the development of a dedicated motor control board with commercially available components. The smallest DC brushless motors were selected as actuators for the bending mechanism, but the available driver board for these motors (SSD04, Namiki Precision Jewel Co., Ltd., 19.6 mm $\times$ 34.4 mm $\times$ 3 mm) does not come in the suitable size for the ingestible modules. Considering the space constraint inside the capsule, a custom control board was developed, optimized, and tested.

Regarding real time communication, the time necessary for sending data from the user interface to the robotic device is one of the important parameters. It takes 21.5 ms to send the longest message of 128 bytes and receive an acknowledgment. However, the typical message to turn on/off the motor requires only 10–20 bytes. The resultant communication can be fast enough to achieve real time operation, also considering that the acceptable time delay is no more than 330 ms for robotic surgery.[20]

This custom board was built by using CC2430 microcontroller (Texas Instrument, USA) as the main controller. To deliver required current to the DC brushless motor, three sets of A3901 dual bridge motor drivers (Allegro MicroSystem, Inc., USA) were mounted. The A3901 motor driver chip is originally intended for a brushed DC motor, but the software commutation algorithm was implemented to control also a DC brushless motor. The dimension of the resulting board was 9.6 mm in diameter and 2.5 mm in thickness. An IEEE 802.15.4 wireless personal area network (WPAN) was introduced as an embedded feature (radio peripheral) of the selected microcontroller.

Controlling brushless DC motors with minimum component usage has been studied in literature.[21–23] Moreover, the preemptive priority pseudokernel approach has been studied[24] so that it can be implemented on the motor control to drive multiple brushless DC motors in real time using one microcontroller instead of utilizing one chip dedicated to each motor. This approach consists of the state-driven code, coroutine, and pooled loop algorithm, which have been demonstrated on the eight-bit microcontroller of CC2430 series. The method of controlling the brushless DC motor can be selected between Back Electro-Motive Force (BEMF) feedback or stepping mode. Maintaining motor position by using position feedback from the motor is not necessary due to the high gear reduction ratio of the motor (337:1), that makes the motor virtually not back-drivable. When the stepping mode is chosen, the DC brushless motors selected for the system (SBL02-06H1PG337 and SBL04-0829PG337) can be driven with the resolution of 0.178°. It should be noted that additional uncertainties will be introduced onto the module actuation due to the fabrication and assembly of other mechanical components.

For the wireless communication, a simple networking scheme consisting of one network coordinator, several network routers, and several end devices were defined. The network coordinator is placed behind the core of user interface which is in charge of sending and receiving commands to/from the end devices. Due to the high rate of the radio signal absorption by human tissues,[25] several network routers can be placed extracorporeally to gain a robust and reliable wireless communication between the user interface and the end devices. From the end devices'

https://doi.org/10.1017/S0263574709990610 Published online by Cambridge University Press

viewpoint, increasing the number of network routers outside the patient may save the power significantly because the adaptive radio transmission feature can keep the transmission power at the lowest level.

5.3. Power management

Instead of using only one module to power the entire configuration of the proposed robot, an embedded power supply in the form of a rechargeable Li–Po (Lithium Polymer) battery is included in each module. The battery capacity carried by each module may differ from one to another depending on the available space inside the module, from 10 mAh to 50 mAh. The continuous driving tests of the 4-mm diameter DC brushless motor (SBL04-0829PG337) at its maximum speed was performed using a 20 mAh Li–Po battery and it lasted up to 17 min. In the surgical application, it is not common for the motors to be driven continuously. Considering the driving load of a typical surgical procedures, it is approximated that the battery should last up to 3 h. A unified distributed power supply is implemented as the energy sharing solution to the proposed system. Furthermore, a particular extended power module can be added as a module of the heterogeneous robotic scheme to lengthen operational duration. Unifying these distributed power supplies simplifies the power management process, but it introduces more difficulties in identifying the power consumption of the individual module.

6. Obtaining the Suitable Topology

As a modular robotic mechanism, it is necessary for the proposed surgical system to define what kinematic chain(s) to assemble the modules into. This section presents the concept of the proposed algorithm to identify the suitable topology and its preliminary results. The algorithm serves to assist in the process of selecting a robot topology given a surgical task and to ensure that all the requirements of the tasks and constraints associated are satisfied by the selected topology for all point in the workspace. For clarity of presentation, the term *topology* is used in this paper to refer to the description of the kinematic chain(s) that define a robot, while the term robot configuration refers to the joint space displacements of the robot.

In this preliminary result, only serial kinematic chains are considered. Interval analysis[26,27] was found to be the suitable fundamental tool of numerical calculation, capable of certifying whether a requirement or constraint is satisfied. In this application, a required workspace is defined as $\mathcal{W}$. This would represent the section in the stomach that the robot has to operate in, e.g. the $Fundus$ or the $Cardia$. The existence of a reference point ($\mathcal{O}$) is assumed. In practice, a structure will be established in the stomach cavity at the start of the procedures which maintains its position relative to the stomach wall. This is done either by applying pressure against the stomach wall or by other means of fastening itself against the stomach wall. The use of a robotic mechanism to press against the stomach wall can also double up as the means of distending the stomach for the surgical procedure. The reference point can be obtained by 3D fluoroscopy.

6.1. Requirements and constraints

Both requirements and constraints are expressed as mathematical equalities or inequalities in the algorithm. Requirements reflect the conditions that need to be satisfied from the point of view of the tasks, such as workspace requirement, tool force requirement, and the necessary resolution of the end-effector motion. Constraints are dictated by the design and the capabilities of the robotic system, such as maximum joint deflection of the modules (joint limits), maximum amount of torque exerted by the motor, resolution of the joint motion as limited by the displacement sensors, the resolution of the control signal, and the performance of the motion control strategy.

6.2. Interval analysis

As mentioned above, interval analysis was utilized as the tool to obtain the suitable topology and to certify that all requirements and constraints are satisfied. There is a vast knowledge related to the study of interval analysis which cannot be explained fully in this paper. Conceptually, the feature that making it important in solving this problem is the nature of the interval arithmetics, where consideration is carried out for all points within the defined range of a variable/parameter, not just by point sampling basis. This provides a very robust and safe (certified) solutions to the numerical calculation involved in this algorithm. By interval arithmetics, a variable x is expressed as an interval $X \in [\underline{x}, \overline{x}]$; where $\underline{x}, \overline{x}$ are the lower and upper bound of the variable. When x is shown to satisfy an inequality, then all continuous values $[\underline{x}, \overline{x}]$ satisfy the inequality. Several main properties are explained below.

Overestimation: Evaluating a function in interval arithmetics may cause overestimation on the resulting bound. This happens when a variable occurs multiple times in a function. As a quick example, let $X = [1, 2]$ and $Y = [3, 4]$, then $X + Y = [4, 6]$. However, numerically evaluating $X - X = [1, 2] - [1, 2] = [-1, 1]$. The overestimation in this case is clear, as obviously $X - X = 0$. It can be observed that overestimation is unavoidable when numerically evaluating an expression, as multiple occurrences of the same variable are taken as independent variables.

Consistency Filtering: This is performed by numerically ensuring the consistency of a variable across one or more equalities/inequalities.[28–31] Interval variables can be initiated with a wide interval and it is possible that only a subset of the values satisfied a given equality/inequality. Filtering techniques numerically remove the subsets of the interval variables/parameters which fail to satisfy these mathematical constraints. These techniques can be used to minimize the effect of overestimation, among other things.

Branch-and-Bound: It is logical to see that if the variables of interest are defined as very wide intervals, it is more difficult to certify whether or not the given mathematical constraints are satisfied. Again, it is likely that only a subset of the intervals satisfies these constraints. Furthermore, overestimation will inflate the interval expressions and makes it more difficult

https://doi.org/10.1017/S0263574709990610 Published online by Cambridge University Press

Table II. Summary of the proposed algorithm.

Function: Evaluate Topology
Input: topology H_i, and the list of all constraints
Output: 1, 0, -1, (if the topology is found to be an inner, boundary, and outer boxes, respectively).

1 Initiliase Workspace $\mathbf{X} = \mathcal{W}$
2 Initialize empty lists $\mathcal{L}_B$.
4 Initialize list $\mathcal{L}$ containing workspace $\mathbf{X}$.
5 **While** ($\mathcal{L}$ not empty)
(a) Extract interval pose $\mathbf{X}$ from $\mathcal{L}$
(b) Evaluate all constraints with $\mathbf{X}$ using interval arithmetics and consistency filtering.
(c) **If X** is an outer box
Return (-1)
Exit *EvaluateTopology*
(e) **Else If X** is a boundary box
(i) If Dimension ($\mathbf{X} > \epsilon_x$)
Bisect $\mathbf{X}$ into $\mathbf{X}(1)$ and $\mathbf{X}(2)$
Add $\mathbf{X}(1)$ and $\mathbf{X}(2)$ to list $\mathcal{L}$.
(ii) Else If Dimension($\mathbf{X} \leq \epsilon_x$)
Add $\mathbf{X}$ to $\mathcal{L}_B$.
(iii) End If
(f) **End If**
6 **End While**
7 **If** ($\mathcal{L}_B$ is empty);
(This means there is no boundary box, i.e., $\mathcal{W}$ is all inner boxes.
Return (1)
8 **Else**
(There are boundary (uncertified) boxes in $\mathcal{W}$;
Return (0)
9 **End If**

to verify whether or not they satisfy the constraints. The *Branch-and-Bound* technique is a loop that bisects the interval variables in turn to numerically evaluate the given constraints through interval arithmetics. When a subset satisfies *all* the constraints, it is labeled as an *inner box*. If a subset fails to satisfied *any* one of the constraints, it is labeled as an *outer box*. When a clear decision cannot be made, the subset of interval variable is labeled a *boundary box*, and is returned to the loop to be bisected further. The bisection process terminates when a threshold dimension (ϵ_x) of the interval boxes is reached.

6.3. The proposed algorithm to obtain the suitable topologies

The proposed concept is to evaluate all possible topologies ($H = \{H_1, H_2, H_3, \ldots H_N\}$) that can be constructed out of the given set of robotic modules, and to identify which topologies are guaranteed to be capable of satisfying all the task requirements once given the robot constraints. To do this, all requirements and constraints are expressed as mathematical equalities/inequalities, and evaluated through interval arithmetics for all values within the desired workspace $\mathcal{W}$. If all points in $\mathcal{W}$ are certified as *inner boxes* to all the constraints, then all the task requirements and design constraints are satisfied, and the topology is capable of carrying out the given surgical task. If any of the points in $\mathcal{W}$ is an *outer box* to any of the constraints, then it is shown that one or more of the requirements or design constraints are not satisfied. The topology is therefore not capable of carrying out the given task. If any subset of the workspace $\mathcal{W}$ remains as a *boundary box* at the end of the *branch-and-bound* loop for a possible topology H_i, then the topology cannot be certified as either capable or incapable of carrying out the given surgical task. The pseudo code summary of the proposed algorithm to evaluate one unique topology H_i out of the list of topologies H is given in Table II.

In this paper, an example specific to the surgical procedure using the developed prototype is defined to illustrate the algorithm. An example of the design of a general-case serial manipulator using the proposed interval analysis algorithm is presented in.[32] Let a desired workspace $\mathcal{W}$ be defined by interval $[P_x, P_y, P_z]$. Variables P_x, P_y, and P_z are interval variables, made up of all values defined by the upper and lower bounds of the variables. The desired workspace $\mathcal{W}$ therefore takes the form of a box. In this example, three homogeneous modules are utilized to actuate a tool tip and it is desired that all points within $\mathcal{W}$ can be achieved. The design limitation is that the bending module can only produce a displacement of $\pm 30°$.

In general cases, the number of possible topologies to be made up by varying the kinematic parameters (the offset link lengths and offset angles) to all possible continuous values would be infinitely large. In this case, however, kinematic parameters can only consist of those values made up by the module dimensions and possible docking orientations. In the proposed algorithm, a list of all possible topologies is generated and each possibility is evaluated by the algorithm summarized in Table II. The design of the homogeneous modules is such that each module is capable of 1 DOF

https://doi.org/10.1017/S0263574709990610 Published online by Cambridge University Press

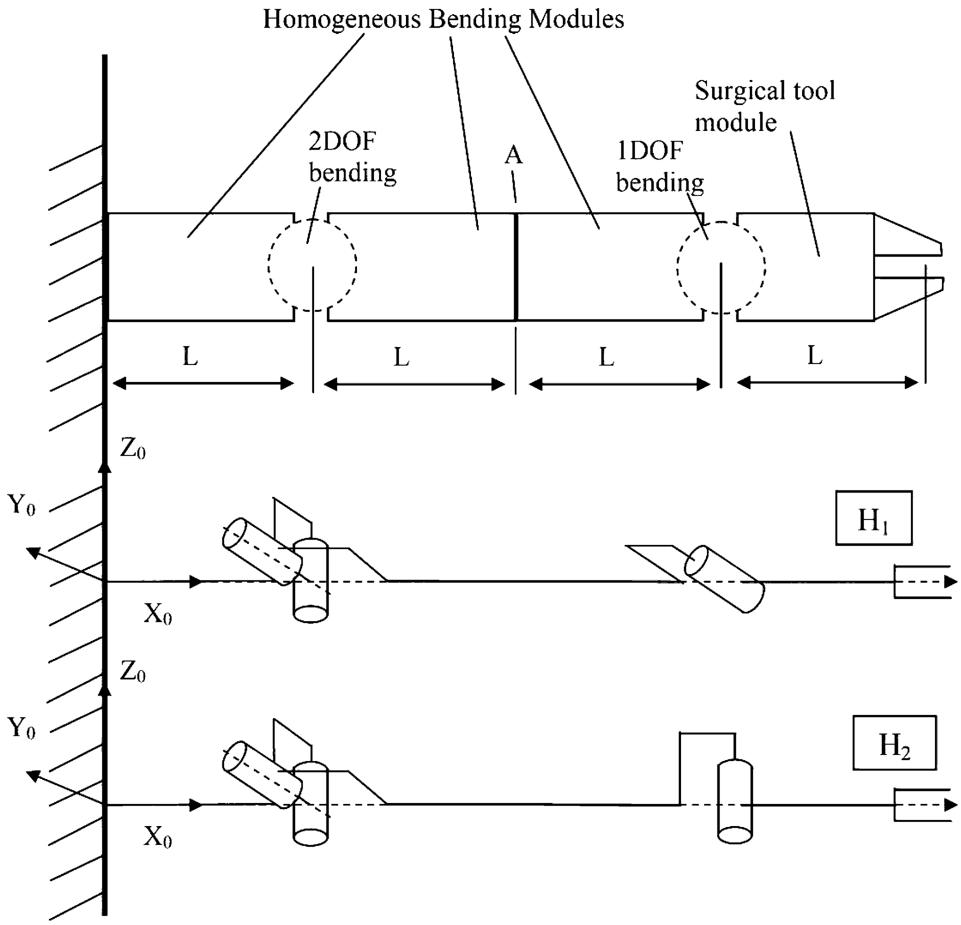

Fig. 12. Possible kinematic chains when using three homogeneous bending modules.

bending on one end of the module and the other end is a magnetic docking mechanism. Two of the modules can be docked together on a single magnetic ball, thus producing a 2 DOF bending mechanism, with intersecting axes of rotation (which are perpendicular to each other), and with a common center of rotation. The homogeneous module design reduces the number of possible combinations in the ways of docking two modules together. The symmetry along the length of the module also means that there can only be two ways to dock two modules together on the unactuated ends, i.e., at 0° and 90° docking orientation. On the actuated end, there is only one way to dock two modules together, i.e., where the axes of rotation of the two modules are perpendicular to each other. Overall, it can be seen that there are only two possible combinations in putting the three bending modules together, as shown in Fig. 12. These two possible topologies differ only in the docking orientation of the modules at connection A (marked in Fig. 12). The topologies shown in Fig. 12 make up all the possible topologies $H = \{H_1, H_2\}$. The base frame shown in Fig. 12 ($[X_0, Y_0, Z_0]$) is the reference frame to be selected on a relatively stable location in the stomach for the surgical procedure. This could be a part of the robotic mechanism that presses against the wall of the stomach to distend the stomach and at the same time provide a relatively stable frame for the robotic mechanism to work in.

In this example, it is desired to verify that $\mathcal{W}$ is achievable given the joint limit. The joint space displacement is described as an interval vector Q, where $Q = [q_1, q_2, q_3]$ and q_1,q_2, q_3 are interval variables. Evaluating a forward kinematics $X = \mathit{ForwardKinematics}(Q)$ (in interval arithmetics) with joint displacement set at the joint limit $\{q_1, q_2, q_3\} \in [-30^\circ, 30^\circ]$, would result in an overestimated end-effector workspace X. Even if it was found that the desired workspace $\mathcal{W}$ is contained within X, no certified conclusion can be drawn on whether this workspace can be achieved by the robot given the joint limits. It is therefore necessary to carry out the inverse kinematics $Q = \mathit{InverseKinematics}(X)$, setting $X = \mathcal{W}$ (the desired workspace), and evaluate whether the resulting Q is contained within $[-30^\circ, 30^\circ]$. It is understood that Q is overestimated. Hence, if an overestimated Q is contained within the joint limits, then it is guaranteed that the entire $\mathcal{W}$ can be achieved with the given joint limits. Naturally, an efficient filtering method is required in order to minimize overestimation so that a certified solution that best reflect the capability of the robot with this specific topology can be obtained.

Depending on the required achievable workspace $\mathcal{W}$, the proposed algorithm evaluates whether topologies H_1 and H_2 satisfy the constraint of the desired workspace being achievable by the robot given the joint displacement limits. The subset of the workspace that is achievable by topology H_1 given the joint limits of $[-30^\circ, 30^\circ]$ calculated through the proposed algorithm can be displayed on a 3D plot as shown in Fig. 13. Note that because inverse kinematics is utilized, then workspace associated with singular configurations of the

https://doi.org/10.1017/S0263574709990610 Published online by Cambridge University Press

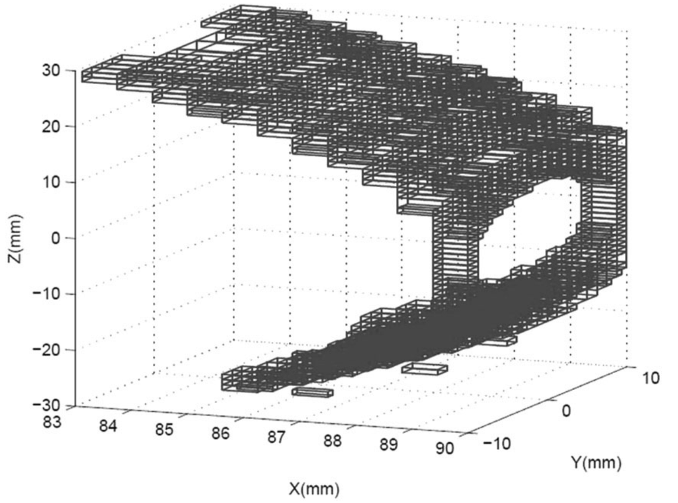

Fig. 13. Reachable workspace by topology H_1, given joint limit of $[-30°, 30°]$.

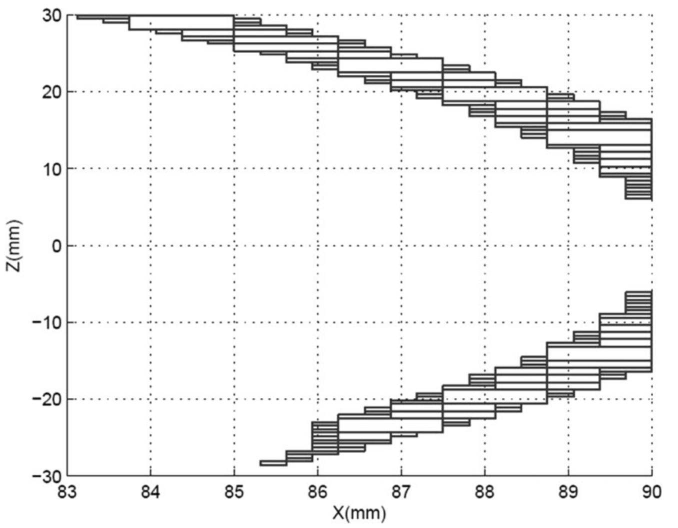

Fig. 14. Two dimensional plot of the achievable workspace, $X_0 - Z_0$ plane on $Y_0 = 0$ of Fig. 13.

manipulator has not been certified as inner boxes. Another constraint is added to evaluate the reachable workspace only through an "elbow down" configuration, i.e., only for positive values of joint q_3. This is done because the manipulator crossing from the "elbow up" to "elbow down" configurations and vice versa, would encounter a singular configuration. For ease and clarity of presentation, a slice of the workspace on $X_0 - Z_0$ plane is presented as 2D plot at $Y_0 = 0$ (Fig. 14).

If the desired workspace is defined as $\mathcal{W} = ([88, 90], [0, 4], [12, 15])^T$ *mm*, then evaluating both topologies (H_1 and H_2) with a joint limit constraint of $\pm 30^o$, will yield a result that both topologies H_1 and H_2 are capable of achieving the given desired workspace.

6.4. Error and uncertainties

Numerical computation through interval analysis is robust to computational *rounding error*. Additionally, any uncertainties in the tasks, in the mechanism design, in robot capabilities, and in kinematic parameters can also be incorporated in the evaluation. This is done by expressing the associated parameters/variables as intervals, instead of real variables, thus reflecting the uncertainties in the width of the interval. For example, the kinematic parameters, such as link lengths/offset distances, can be expressed as intervals, bounded within the minimum and maximum possible values due to the uncertainties. An example of this type of uncertainties is the fabrication tolerances. Another example is related to the uncertainties associated with the docking mechanism, which can result in an unwanted angular offset if the modules were not connected properly. This can be incorporated by expressing the offset angles in the kinematic parameters as intervals. This guarantees that when a workspace $\mathcal{W}$ is certified to satisfy all constraints, they do so even as all these uncertainties are taken into account.

7. Discussion

In the prototype design, the size specification (11 mm by 26 mm) could not be achieved mainly due to the size limitation of available components on markets (e.g., the motors and the battery). However, it would be better to start designing the prototypes as close as possible to the desired specification and then miniaturize them further to the preferred size of 8 mm by 16 mm.

For the reconfiguration of the topology, the docking and undocking mechanism, the communication between the modules and the calculation of suitable topologies are key technologies to be developed. The module dedicated for docking/undocking using permanent magnets is under development,[19,33] intended to be integrated in the modular scheme. The next stage is implementing the undocking mechanism to the current module, and the design is in progress.

The electrical connection for the communication between modules can be achieved by implementing connector parts to each design. When the internal communication is established, the sequence of the modules (i.e., the robotic topology) can be identified because the control boards can then exchange information between the connected modules. The desired structure can be achieved through reconfiguration by repeated docking and undocking until the desired topology is confirmed by the internal communication between the modules.

Unlike the commercially available surgical robots today, the proposed surgical robot is completely inserted in the body. Within this study, further medical evaluation will be carried out to investigate the risks associated with this new approach of surgical procedures. Up to this moment, in addition to the risks associated with conventional surgery, it has been identified that this proposed approach may also introduce foreseeable difficulties in extracting the modules from the body. In the case where a module is stuck in the small intestine due to a narrowed passage that some patients may have, another operation to remove the retained module may be needed.

The patient selection criteria for the proposed surgical system can be learned from the preceding study on the capsule endoscopy. Before being approved as a commercial medical device, preclinical and clinical studies are necessary for this kind of robots. Preclinical study includes the

https://doi.org/10.1017/S0263574709990610 Published online by Cambridge University Press

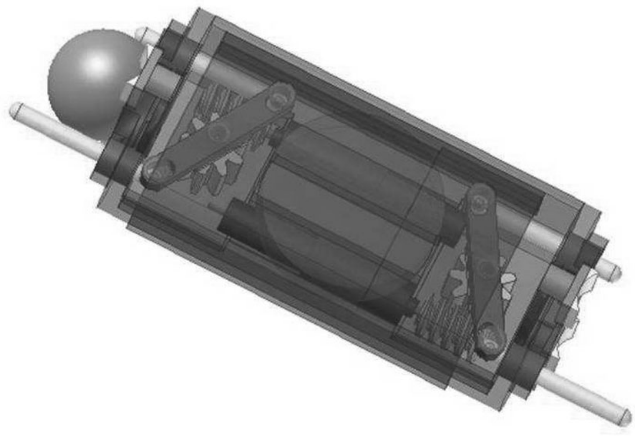

Fig. 15. New design of homogeneous bending module prototype, more compact with two motors per bending module. This allows bending actuation on both ends of the module.

characterization of the device, performance tests, and safety tests. For example, the material of the parts of the modules that come into contact with the human body/organ must be biocompatible and its resistance to the associated body environment should be confirmed. These studies will need to be conducted considering the difference between commercial capsule endoscope and the proposed surgical system.

The topology and workspace analysis of the homogeneous modules demonstrated a reachable workspace that is shell-like in its volume (Fig. 13 and Fig. 14). This is determined by the serial configuration of the manipulator as well as by the $\pm 30^{\circ}$ joint displacement limits for the modules. To increase the thickness of the shell-like volume of the workspace, given the same joint displacement limits, it is necessary to utilize a larger number of bending modules. It can be seen, however, that despite the limitation in the range of motion, the homogeneous design offer the advantages of simpler computational model through the use of uniform modules across the entire topology and the compactness of having 2 DOF motion at one joint through the use of intersecting axes of bending and a common center of rotation. A newer version of the module is being developed, where two motors are fitted into one bending modules, thus allowing an actuated joint at each end of the bending module (Fig. 15), further increasing the compactness of the design.

8. Conclusions and Future Work

An endoluminal surgical robotic system has been proposed and its first target has been defined as the diagnosis and intervention of early stomach cancer located in the upper side of the stomach. A modular approach was selected to overcome the narrow passages of various segments of the the GI tract. Reconfigurability was identified as an important feature to allow the assembly of the robots within the GI tract and passage through the various segments of the tract. Based on the proposed robotic schemes, two approaches of modular designs with structural functions were proposed and their prototypes fabricated.

The miniaturized motor control board was developed specifically for the implementation in the small robotic module within the requirement of its operating environment. The motor control methods and the power management were investigated. The interval-based constraint satisfaction algorithm was developed to determine the suitable topologies of the reconfigurable robot given the task requirements and performance constraints. In this paper, the homogeneous approach has been selected as an example. It can be seen that the homogeneous approach provides simpler kinematic structures compared to the heterogeneous approach. Being able to use different types modules, with different number of docking terminals at different locations of the module would allow more complex kinematic structures to be realized. This may be necessary if several chains of arms or support legs are required, for example, when several end-effectors are required to operate simultaneously. This would obviously increase the number of possibilities in the design algorithm. While the design algorithm is capable of handling the heterogeneous approach, it would then be necessary to properly define the design constraints to be used in evaluating the desired topologies.

Future work involves the integration of the various miniaturized components and experimentation of the reconfigurable modular robot in a stomach model. The magnetic self-assembly has been studied by another group using a stomach model made of acrylic glass filled with water[19] and that study will be integrated to the presented study. Moreover, a stomach simulator is available for the assembly, disassembly and reconfiguration tests with the simulated peristaltic motion.[34] The homogeneous scheme has the priority to the self-assembly test and the topology planning, while the heterogeneous scheme has the priority to the study on the reconfiguration.

Acknowledgments

This work was supported in part by the European Commission, in the framework of the ARES Project(Assembling Reconfigurable Endoluminal Surgical system). The authors would like to thank Professor Alfred Cuschieri for his medical consultancy. The authors are grateful to Mr. Nicodemo Funaro for the manufacturing of the prototypes and Ms. Sara Condino for her invaluable technical support.

References

1. A. Cuschieri, "Laparoscopic surgery: Current status, issues and future developments," *Surgeon* **3**(3), 125–138 (Jun. 2005).
2. A. Moglia, A. Menciassi, M. Schurr and P. Dario, "Wireless capsule endoscopy: From diagnostic devices to multipurpose robotic systems," *Biomed. Microdevices* **9**, 235–243 (2007).
3. M. Quirini, A. Menciassi, S. Scapellato, C. Stefanini and P. Dario, "Design and fabrication of a motor legged capsule for the active exploration of the gastrointestinal tract," *IEEE/ASME Trans. Mechatron.* **13**, 169–179 (2008).
4. L. Phee, D. Accoto, A. Menciassi, C. Stefanini, M. Carrozza and P. Dario, "Analysis and development of locomotion devices for the gastrointestinal tract," *IEEE Trans. Biomed. Eng.* **49**, 613–616 (2002).
5. M. Sendoh, K. Ishiyama and K. Arai, "Fabrication of magnetic actuator for use in a capsule endoscope," *IEEE Trans. Magn.* **39**(5), 3232–3234 (2003).
6. N. Ng Pak, R. Webster III, A. Menciassi and P. Dario, "Electrolytic Silicone Bourdon Tube Microactuator for Reconfigurable

Surgical Robot," *Proceedings IEEE International Conference Robotics and Automation*, (2007) pp. 3371–3376.
7. P. Dario, M. Carrozza, C. Stefanini and S. D'Attanasio, "A mobile microrobot actuated by a new electromagnetic wobble micromotor," *IEEE/ASME Trans. Mechatron.* **3**(1), 9–16 (1998).
8. S.-K. Park, K.-I. Koo, S.-M. Bang, J.-Y. Park, S.-Y. Song and D.-G. Cho, "A novel microactuator for microbiopsy in capsular endoscopes," *J. Micromech. Microeng.* **18**(2), 25 032–0 (2008).
9. A. Lehman, M. Rentschler, S. Farritor and D. Oleynikov, "The current state of miniature in vivo laparoscopic robotics," *J. Robot. Surg.* **1**, 45–49 (2007).
10. S. Giday, S. Kantsevoy and A. Kalloo, "Principle and history of natural orifice translumenal endoscopic surgery (notes)," *Minim. Invasive Ther. Allied Technol.* **15**(6), 373–377 (2006).
11. "The ares (assembling reconfigurable endoluminal surgical system)," Project Website http://www.ares-nest.org, 2006.
12. M. Yim, W. Shen, B. Salemi, D. Rus, M. Moll, H. Lipson, E. Klavins and G. Chirikjian, "Modular self-reconfigurable robot systems [Grand Challenges of Robotics]," *IEEE Robot. Autom. Mag.* **14**(1), 865–872 (Mar. 2007).
13. S. Murata and H. Kurokawa, "Self-reconfigurable robots," *IEEE Robot. Autom. Mag.* 71–78 (Mar. 2007).
14. E. Yoshida, S. Murata, S. Kokaji, K. Tomita and H. Kurokawa, "Micro self- reconfigurable modular robot using shape memory alloy," *J. Robot. Mechatron.* **13**(2), 212–219 (2001).
15. World Health Organisation, "Fact sheet n.297," Online: http://www.who.int/ mediacenter/factsheets/ fs297, 2006.
16. M. Pesic, A. Karanikolic, N. Djordjevic, V. Katic, Z. Rancic, M. Radojkovic, N. Ignjatovic and I. Pesic, "The importance of primary gastric cancer location in 5-year survival rate," *Archive Oncol.* **12**, 51–53 (2004).
17. J. Henry, G. O'Sullivan and A. Pandit, "Using computed tomography scans to develop an ex-vivo gastric model," *World J. Gastroenterol.* **13**(9), 1372–1377 (Mar. 2007).
18. K. Harada, E. Susilo, N. Ng Pak, A. Menciassi and P. Dario, "Design of a Bending Module for Assembling Reconfigurable Endoluminal Surgical System,' *Proceedings the 6th International Conference International Society of Gerontechnology (ISG'08)*, Pisa, Italy (Jun. 4–7, 2008) pp. ID–186.
19. Z. Nagy, R. Oung, J. J. Abbott and B. J. Nelson, "Experimental Investigation of Magnetic Self-Assembly for Swallowable Modular Robots," *Proceedings of IEEE/RSJ International Conference on Intelligent Robots and Systems*, St. Louis, Missouri (Sep. 22–26, 2008) pp. 1915–1920.
20. J. Marescaux, J. Leroy, M. Gagner, F. Rubino, D. Mutter, M. Vix, S. Butner and M. K. Smith, "Transatlantic robot-assisted telesurgery," *Nature* **413**, 379–380 (2001).
21. A. Hapenciuc, V. Catalin and P. Svasta, "Sensorless Brushless Motor Controller with N-MOS Technology,' *International Spring Seminar on Electronics Technology (ISSE)*, (2007) pp. 477–481.
22. J. Shao, "A novel microcontroller-based sensorless brushless DC (BLDC) motor drive for automotive applications," *IEEE Trans. Indus. Appl.* **39**(6), 1734–1740 (Nov. 2003).
23. J. Shao, "An improved microcontroller-based sensorless brushless DC (BLDC) motor drive for automotive fuel pump," *IEEE Indus. Appl. Soc. (IEEE-IAS)*, 2512–2517 (2005).
24. E. Susilo, P. Valdastri, A. Menciassi and P. Dario, "A miniaturized wireless control platform for robotic capsular endoscopy using advanced pseudokernel approach," *accepted to Sens. Actuators A Phys.* **156**(1), 49–58 (2009).
25. K. Shibata, T. Nagato, T. Tsuji and K. Koshiji, "Energy transmission transformer for a wireless capsule endoscope: Analysis of specific absorption rate and current density in biological tissue," *IEEE Trans. Biomed. Eng.* **55**(7), 1864–1871 (Jul. 2008).
26. R. Moore, *Interval Analysis* (Prentice-Hall, Englewood Cliffs, New Jersey, 1966).
27. E. Hansen and G. Walster, *Global Optimization Using Interval Analysis*, 2nd ed. (Marcel Dekker, New York, 2004).
28. F. Benhamou, F. Goualard and L. Granvilliers, "Revising Hull and Box Consistency," *Proceedings of the International Conference on Logic Programming*, Las Cruces, USA (1999) pp. 230–244.
29. M. Collavizza, F. Delobe and M. Rueher, "Comparing partial consistencies," *Reliable Comput.* **5**, 1–16 (1999).
30. O. Lhomme, "Consistency Techniques for Numeric CSPs," *Proceedings of International Joint Conferences on Artificial Intelligence (IJCAI)*, Chambery, France (Aug. 1993) pp. 232–238.
31. A. Neumaier, *Interval Methods for Systems of Equations* (Cambridge University Press, London, 1990).
32. D. Oetomo, D. Daney and J.-P. Merlet, "Design strategy of serial manipulators with certified constraint satisfaction," *IEEE Trans. Robot.* **25**(1), 1–11 (Feb. 2009).
33. Z. Nagy, J. Abbott and B. Nelson, "The Magnetic Self-Aligning Hermaphroditic Connector: A Scalable Approach for Modular Microrobotics," *Proceedings IEEE/ASME International Conference Advanced Intelligent Machatronics*, Zurich, Switzerland (2007) pp. 1–6.
34. A. Menciassi, P. Valdastri, K. Harada and P. Dario, "Single and Multiple Robotic Capsules for Endoluminal Diagnosis and Surgery," *Proceedings of IEEE/RAS-EMBS International Conference on Biomedical Robotics and Biomechatronics*, (Oct. 19–22, 2008) pp. 238–243.

https://doi.org/10.1017/S0263574709990610 Published online by Cambridge University Press